Strongly Correlated Superconductivity and Pseudogap Phase near a Multiband Mott Insulator

Massimo Capone,[1,2] Michele Fabrizio,[3,4] Claudio Castellani,[2] and Erio Tosatti[5,4,6]

[1]*Enrico Fermi Center, Rome, Italy*

[2]*Università di Roma "La Sapienza" and Istituto Nazionale per la Fisica della Materia (INFM), SMC and UDR Roma 1, Piazzale Aldo Moro 2, I-00185 Roma, Italy*

[3]*International School for Advanced Studies (SISSA), and Istituto Nazionale per la Fisica della Materia (INFM) UDR-Trieste SISSA, Via Beirut 2-4, I-34014 Trieste, Italy*

[4]*The Abdus Salam International Centre for Theoretical Physics (ICTP), P.O. Box 586, I-34014 Trieste, Italy*

[5]*International School for Advanced Studies (SISSA), and INFM Democritos National Simulation Center, Via Beirut 2-4, I-34014 Trieste, Italy*

[6]*Laboratoire de Mineralogie-Cristallographie de Paris, Universite Pierre et Marie Curie, 4 Place Jussieu, 75252 Paris, France*

(Received 31 December 2003; published 22 July 2004)

Near a Mott transition, strong electron correlations may enhance Cooper pairing. This is demonstrated in the dynamical mean field theory solution of a twofold-orbital degenerate Hubbard model with an inverted on-site Hund rule exchange, favoring local spin-singlet configurations. Close to the Mott insulator (which here is a local version of a valence bond insulator) a pseudogap non-Fermi-liquid metal, a superconductor, and a normal metal appear, in striking similarity with the physics of cuprates. The strongly correlated *s*-wave superconducting state has a larger Drude weight than the corresponding normal state. The role of the impurity Kondo problem is underscored.

DOI: 10.1103/PhysRevLett.93.047001 PACS numbers: 74.20.Mn, 71.10.Hf, 71.27.+a, 71.30.+h

How superconductivity emerges so spectacularly out of a weakly doped Mott insulator is one of the fascinating and still controversial aspects of high T_c cuprate superconductors. A novel *strongly correlated superconductivity* (SCS) scenario has been recently proposed [1] which deals with an ultimately related basic issue, namely, the conditions under which Cooper pairing can be *enhanced*, rather than depressed, by strong electron repulsion. The key of the SCS proposal is the presence of a pairing interaction term J, which is weak but is not suppressed by the strong short-range repulsion U. This is realized by any attraction which involves mainly spin and orbital degrees of freedom, which are not frozen near a Mott metal-insulator transition (MIT). In addition, close to the MIT, correlations slow down electron motion so much that the effective quasiparticle bandwidth becomes extremely small $W_{\rm qp} \ll W$, W being its uncorrelated value. In these conditions, the pairing attraction can eventually equal the quasiparticle bandwidth $J \sim W_{\rm qp}$. That drives the system to an intermediate-strong coupling superconducting regime where the *maximum* superconducting gap $\Delta \sim J$ is reached, as opposed to the much smaller uncorrelated BCS value $\Delta_{\rm BCS} \sim W \exp(-W/J)$. A first theoretical realization of SCS was demonstrated in Refs. [1,2] by a dynamical mean field theory (DMFT) [3] solution of a threefold degenerate model for tetravalent fullerides. It was shown that a narrow SCS region arises next to the MIT, and is indeed characterized by a superconducting gap 3 orders of magnitude larger than the value one would obtain for the same attraction in the absence of correlation.

DMFT maps a lattice model onto an Anderson impurity (AI) model subject to a self-consistency condition. Within this mapping SCS emerges [2] through a competition between Kondo screening of the orbitally degenerate impurity (leading to a normal Fermi-liquid) and an intraimpurity mechanism which forms a local nondegenerate singlet [a kind of local resonating valence bond (RVB) state [4]]. This mechanism requires orbital degeneracy and an effective inversion of Hund's rules, both ingredients present in the model of Ref. [1]. More recently, a simpler AI model with only twofold orbital degeneracy was shown by Wilson numerical renormalization group (NRG) to display anomalous properties [5], suggesting its lattice generalization as a new candidate for a SCS.

In this Letter, we present a detailed DMFT analysis that confirms this expectation, exploiting the lower degeneracy for a wider and more revealing study. We consider an infinite coordination Bethe lattice and solve the AI by exact diagonalization. The model reads [5]

$$\hat{H} = -t \sum_{\langle ij\rangle,a,\sigma} c^{\dagger}_{i,a\sigma} c_{j,a\sigma} + \text{H.c.} + \frac{U}{2}\sum_i n_i^2 + \hat{H}_J, \qquad (1)$$

where $c^{\dagger}_{i,a\sigma}$ creates an electron at site i in orbital $a = 1, 2$ with spin σ, while $n_i = \sum_{a,\sigma} c^{\dagger}_{i,a\sigma} c_{i,a\sigma}$ is the on-site occupation number. The on-site Hund's rule exchange is

$$\hat{H}_J = -2J \sum_i (T^2_{i,x} + T^2_{i,y}), \qquad (2)$$

where $T_{i,\alpha} = 1/2 \sum_{a,b} \sum_{\sigma} c^{\dagger}_{i,a\sigma} (\hat{\tau}^{\alpha})_{ab} c_{i,b\sigma}$ are the pseudospin 1/2 operators, and $\hat{\tau}^{\alpha}$ ($\alpha = x, y, z$) the Pauli matrices. The electronic states of the isolated site with n electrons are labeled by total spin and pseudospin, S and T, and their z components, and have energies $E(n, S, S_z, T, T_z) = Un^2/2 - 2J[T(T+1) - T_z^2]$. For $n = 2$,

 0031-9007/04/93(4)/047001(4)$22.50

the configurations allowed by the Pauli principle are a spin triplet orbital singlet ($S = 1$ and $T = 0$) and a spin singlet orbital triplet ($S = 0$ and $T = 1$), split by $\hat{H}_J$. If $J < 0$, standard Hund's rules, the spin triplet has the lowest energy. Here we consider the less common case of $J > 0$, where the lowest energy configuration has $S = 0$, $T = 1$, and $T_z = 0$. This inversion of Hund's rules may, for instance, mimic a dynamical $e \otimes E$ Jahn-Teller effect [1,2]. Here it just represents a generic mechanism for on-site spin-singlet pairing. Indeed, for $U = 0$ and $J \ll W$, the ground state of (1) is an s-wave BCS superconductor with pairs condensed in the $S = 0$, $T = 1$, and $T_z = 0$ channel. The energy gap is $\Delta \sim W \exp(-1/\lambda)$, where $\lambda = 2JN_F$ is the dimensionless superconducting coupling, and N_F the density of states (DOS) at the Fermi energy per spin and orbital. In this regime, a finite $U \ll W$ introduces a "Coulomb" pseudopotential $\mu_* = UN_F$ that opposes superconductivity, eventually suppressed for $U > 2J$ in favor of a normal metal ground state. For larger $U \geq U_c \sim W$, the model (1) undergoes a MIT for all integer fillings $\langle n \rangle = 1, 2, 3$. We could generally expect the superconducting gap to decrease monotonically as a function of U, the superconductor either turning directly into a Mott insulator (for $\lambda \sim 1$), or (when $\lambda \ll 1$) first into a metal, and then into the insulator. This is indeed what we find for $\langle n \rangle = 1$ (equivalent to $\langle n \rangle = 3$ by particle-hole symmetry) and λ ranging from 0.1 to 0.6. The picture is, however, richer in the half-filled $\langle n \rangle = 2$ case, as reported in Fig. 1. Here the standard superconductor evolves continuously into the SCS regime. If λ is large (e.g., $J/W = 0.15$), Δ decreases with increasing U, as in a BCS superconductor, until a weakly *first order* transition to our local-RVB insulator occurs [6]. For smaller λ, however, the dependence of Δ on U is non-

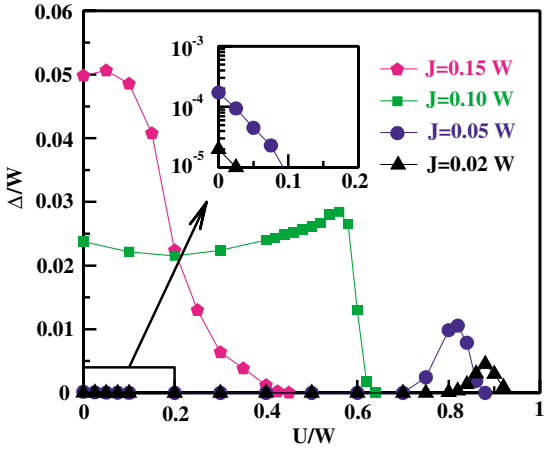

FIG. 1 (color online). Superconducting gap for $\langle n \rangle = 2$ as a function of on-site repulsion for fixed coupling $J = \lambda/(2N_F)$. Increasing repulsion spoils superconductivity at large coupling. Superconductivity is instead strongly enhanced close to the Mott transition at weak coupling. The inset shows the weak coupling regime on an expanded scale, showing a much smaller gap at small U compared with SCS at large U.

monotonic, and the initial drop for small U is followed by a rise. Finally, for the smallest values of λ, the weak-U superconductor first turns into a metal but, just before the MIT, reverts back to a superconductor, as in the three-band SCS model of Ref. [1]. Here, too, the superconducting gap reaches values much larger than those attained for the same pairing attraction λ (compare the inset and the right-hand side of Fig. 1).

The appearance of SCS in (1) for $\langle n \rangle = 2$ strongly supports the AI analysis [5]. Indeed, as U increases, the quasiparticle bandwidth, which is the AI effective Kondo temperature T_K, is gradually suppressed by the dropping quasiparticle residue $Z \ll 1$, $T_K \sim ZW$. At the same time, we expect J to remain unrenormalized [1]. In fact, $\hat{H}_J$ splits multiplets with the same n, and that can happen without opposing U, which just freezes charge fluctuations regardless of either spin or orbital degrees of freedom. As Z decreases, the AI enters the critical region around its unstable fixed point [5] at a critical $T_K^{(c)} \sim J$. For $T_K > T_K^{(c)}$, the AI is in the Kondo screened regime, while for $T_K < T_K^{(c)}$ an intraimpurity singlet forms thanks to the inverted exchange J. At the fixed point, the two effects balance exactly, leading to a residual entropy $\ln\sqrt{2}$. The remaining impurity degrees of freedom are quenched at a larger temperature $T_+ \sim \max(T_K, J)$. $T_- \sim |T_K - T_K^{(c)}|^2/T_K^{(c)}$ measures the deviation from the fixed point behavior. It was argued in Ref. [5] that DMFT self-consistency should turn this AI instability into a true bulk one, most likely implying superconductivity. This is now confirmed by our DMFT analysis. s-wave superconductivity opens up a new screening route which freezes the residual entropy, otherwise quenched only below T_- [5]. This suggests that (i) the energy scale which controls superconductivity should be related to $T_+ - T_-$; (ii) the onset of superconductivity should be accompanied by a kinetic energy gain, as Kondo screening implies. A kinetic energy (or, more accurately, band energy) gain may be regarded as a signal of SCS (as opposed to BCS where kinetic energy rises), and that should be reflected by the behavior of the Drude weight. In Fig. 2, we show for $J = 0.05W$ the Drude weight of the stable superconducting solution for $0.7 \leq U/W \leq U_c$ (here the Drude weight is the strength of the superfluid peak), in comparison with that of the *unstable* metallic solution (obtained disallowing superconductivity), taken to represent the normal phase. Figure 2 shows a large increase of Drude weight with superconductivity, an occurrence also predicted in high T_c superconductor models [7,8] and actually observed in cuprates [9]. Here the unstable metal Drude weight actually appears to vanish at $U_* < U_c$. As we shall show, this reflects the opening of a pseudogap at the chemical potential before the MIT.

Additional physical insight is gained by analyzing the DOS in the strongly correlated region $U/W > 0.7$. Within DMFT, the DOS in this region of parameters displays

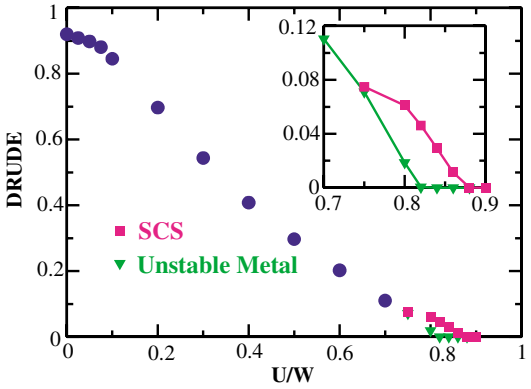

FIG. 2 (color online). Drude weight as a function of U at $J = 0.05W$. SCS points: superconducting solution; unstable metal points: metastable solution with superconducting order parameter forced equal to zero. Note the very large Drude weight increase in the SCS pocket (magnified in the inset).

three features: Two high-energy Hubbard bands and a low-energy quasiparticle feature. Figure 3 displays the evolution of the DOS of the normal state solution with increasing U, and shows that a pseudogap opens within the low-energy peak. A similar pseudogap appeared also in the NRG solution of the AI of Ref. [10], where it was argued that the low-energy DOS around the unstable fixed point is well described by

$$\rho(\omega) = \frac{\rho_0}{2}\left(\frac{T_+^2}{\omega^2 + T_+^2} \pm \frac{T_-^2}{\omega^2 + T_-^2}\right). \qquad (3)$$

where ρ_0 is the noninteracting DOS, and plus/minus refers to the Kondo screened/unscreened phase. We find that (3) fits very well the low-frequency behavior of the

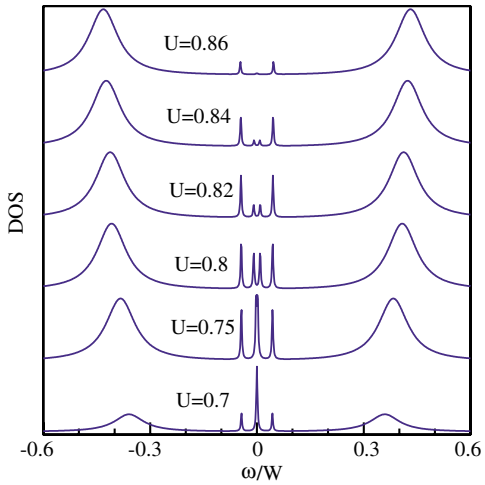

FIG. 3 (color online). Single-particle DOS at $J = 0.05W$ of the metallic solution for U close to the MIT (superconductivity disallowed between $U = 0.7$ and $U_c \simeq 0.88$). Note the pseudogap within the low-energy quasiparticle peak coexisting with the high-energy Hubbard bands. The spiky nature of the spectrum in an artifact introduced by the discrete Lanczos diagonalization.

DMFT results [11]. Equation (3) implies that $\rho(0) = \rho_0$ in the Kondo screened regime, which is compatible with a Fermi liquid with $\mathrm{Im}\,\Sigma(\omega) \sim \omega^2$. On the contrary, we find DOS values of $\rho(0) = \rho_0/2$, at $T_- = 0$, and $\rho(0) = 0$ in the pseudogap phase, which imply a singular behavior of the self-energy, i.e., a non-Fermi-liquid. The best-fit values of T^+ and T^- for $J = 0.05W$ are shown in Fig. 4, and compared with the superconducting gap Δ. The maximum of Δ almost coincides with the vanishing of T_-, which corresponds to the AI unstable fixed point. Figure 4 suggests a scenario which shares some similarities to the quantum critical point [12] and the gauge theory-slave boson [13] pictures of cuprates. For temperatures T above T_c (presumably of order Δ) but below T_-, the normal phase is a Fermi liquid for $U < U_*$, and a non Fermi-liquid pseudogap phase for $U_c > U > U_*$. For $T_- < T < T_+$, both the narrow Fermi-liquid quasiparticle peak and the pseudogap should be washed out, leaving a broader resonance reflecting the properties of the non Fermi-liquid AI unstable fixed point. The resonance will eventually disappear altogether above T_+. Close to the MIT, the unstable metal and the stable superconductor have almost the same energy and very similar DOS, but for the presence of a very small superconducting gap. From this point of view, the pseudogapped unstable phase plays a role similar to the staggered flux phase within the SU(2) invariant slave-boson description of the t-J model, and may therefore be thought of as a phase with broken symmetry in the particle-hole or in the particle-particle channels, where the full symmetry is restored by fluctuations [13]. We note here that (a) superconductivity is not an accidental route which the lattice system takes to rid itself of competition among other phases, but is one of the predetermined instabilities of the AI; (b) attempts to uncover the fixed point by suppressing superconductivity would likely spoil the fixed point or unveil other instabilities of the lattice model.

The analogy with high T_c cuprates becomes even more suggestive when we analyze the phase diagram away from

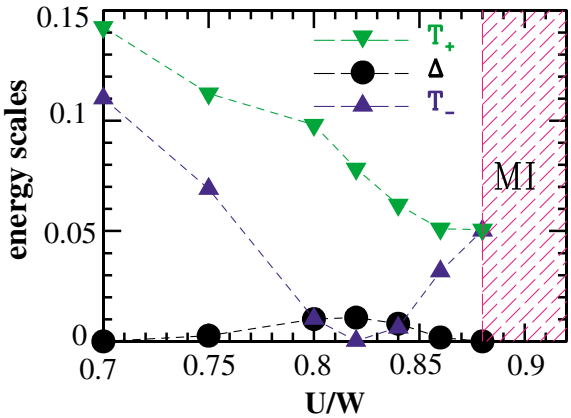

FIG. 4 (color online). Behavior of the relevant energy scales (defined in the text) close to the MIT for $J/W = 0.05$ as function of U/W.

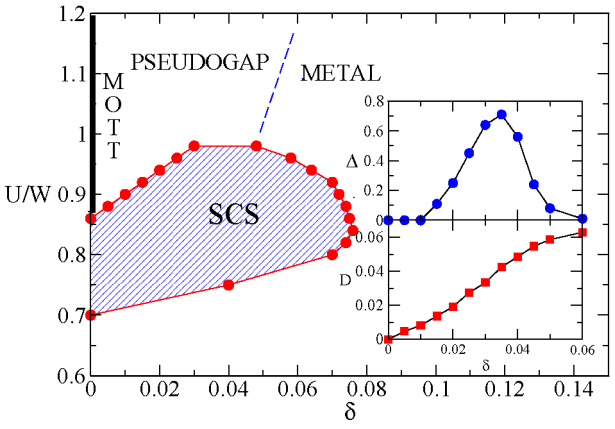

FIG. 5 (color online). Phase diagram as a function of U/W and doping $\delta = n - 2$ at $J = 0.05W$. The thick vertical line marks the singlet Mott insulator. The inset shows, for $U = 0.92W$, the superconducting gap Δ divided by a factor 10^{-3} and the Drude weight D (normalized to the noninteracting value) as functions of doping δ.

half filling, and follow the fate of superconductivity upon doping. SCS extends (Fig. 5) into a superconducting pocket away from $\langle n \rangle = 2$. When we dope the singlet Mott insulator just above the MIT, a pseudogap metallic phase is encountered first, followed by a narrow superconducting region which finally gives way to a normal metal (inset of Fig. 5), in remarkable similarity to the phase diagram of high T_c cuprates. Striking is also the similarity in the Drude weight (inset), which is zero in the Mott insulator at half filling and increases almost linearly upon doping. The phase diagram of Fig. 5 again agrees with the AI analysis [10], which showed that the unstable fixed point still exists away from half filling.

In the alkali fulleride models, which provide our prime examples of SCS, the physics which leads to $J > 0$ and spin pairing is Jahn-Teller, i.e., a conventional phonon effect [1,2,14]. Future experiments to test the SCS scenario by comparing Drude weights in the presence and in the absence of superconductivity should be actively considered in trivalent fullerides such as $K_3NH_3C_{60}$ [15]. These materials are of extraordinary importance, for they show a similar "universal" contiguity between superconductivity and Mott insulating behavior as the high T_c cuprates do, albeit with different physical ingredients. When dealing with spectroscopies, one should keep in mind that there are now two low-energy scales, T_+ and T_-. That makes, e.g., photoemission data such as the recent ones on K_3C_{60} [16] especially difficult to analyze. In the SCS region, coherent bandlike dispersion should occur with a reduced bandwidth of order $2T_+$, a scale which *remains finite* across the MIT, even though the system is strongly correlated. The true quasiparticle peak will instead become extremely narrow, of order T_-, or even disappear in the pseudogap regime. In view of that, we believe that the data [16] are actually compatible with the SCS scenario.

The underlying degenerate Kondo physics offers a new intriguing insight in strongly correlated superconductivity. The onset of bulk coherence close to a MIT may involve a hierarchy of energy scales, $T_- < T_+$ and Δ. The latter is the most sought after as it marks the onset of lattice long-range order. On the contrary, T_+ and T_- have their clearest meaning in the AI, which displays a two-stage quenching of the impurity entropy.

We are grateful to L. De Leo and to J. E. Han for sharing with us their results prior to publication, and to P. Nozières, E. Cappelluti, G. E. Santoro, and M. Lueders for illuminating discussions. This work has been supported by MIUR Cofin 2003, MIUR FIRB RBAU017S8R004, FIRB RBAU01LX5H, and by INFM Progetto Calcolo Parallelo.

[1] M. Capone, M. Fabrizio, C. Castellani, and E. Tosatti, Science **296**, 2364 (2002).
[2] M. Capone, M. Fabrizio, and E. Tosatti, Phys. Rev. Lett. **86**, 5361 (2001).
[3] A. Georges *et al.*, Rev. Mod. Phys. **68**, 13 (1996).
[4] P.W. Anderson, Science **235**, 1196 (1987).
[5] M. Fabrizio, A. F. Ho, L. De Leo, and G. E. Santoro, Phys. Rev. Lett. **91**, 246402 (2003).
[6] This result is consistent with those reported for a threefold degenerate case by J. E. Han, O. Gunnarsson, and V. H. Crespi, Phys. Rev. Lett. **90**, 167006 (2003).
[7] J. E. Hirsch, Physica (Amsterdam) **199C**, 305 (1992).
[8] G. Baskaran, Int. J. Mod. Phys. B **14**, 2117 (2000).
[9] H. J. A. Molegraaf, C. Presura, D. Van Der Marel, P. H. Kes, and M. Li, Science **295**, 2239 (2002).
[10] L. De Leo and M. Fabrizio, cond-mat/0402121 [Phys. Rev. B (to be published)].
[11] In our Bethe lattice, the fit works better with semicircular DOS's rather than Lorentzians.
[12] C. M. Varma, Phys. Rev. B **55**, 14554 (1997); C. Castellani, C. Di Castro, and M. Grilli, Z. Phys. B **103**, 137 (1997); S. Sachdev, Rev. Mod. Phys. **75**, 913 (2003), and references therein.
[13] See, e.g., P. A. Lee, Physica (Amsterdam) **388C**, 7 (2003), and references therein.
[14] Our model is equivalent to an $e \otimes E$ Jahn-Teller model in the antiadiabatic limit. We believe, however, that a realistic treatment of the phonons would provide similar results. We are grateful to Dr. J. E. Han for discussion and correspondence about this point.
[15] O. Zhou *et al.*, Phys. Rev. B **52**, 483 (1995); H. Tou *et al.*, Phys. Rev. B **62**, R775 (2000); S. Margadonna *et al.*, Europhys. Lett. **56**, 61 (2001).
[16] W. L. Yang *et al.*, Science **300**, 303 (2003); A. Goldoni *et al.*, Phys. Rev. B **58**, 11023 (1998).